Optical Fiber Technology 15 (2009) 172–180

Contents lists available at ScienceDirect

Optical Fiber Technology

www.elsevier.com/locate/yofte

Large signal-to-noise-ratio enhancement of ultrashort pulsed optical signals using a power-symmetric Nonlinear Optical Loop Mirror with output polarisation selection

O. Pottiez [a,*], B. Ibarra-Escamilla [b], E.A. Kuzin [b]

[a] Centro de Investigaciones en Óptica, Loma del Bosque 115, Col. Lomas del Campestre, 37150 León, Gto, Mexico
[b] Instituto Nacional de Astrofísica, Óptica y Electrónica (INAOE), Departamento de Óptica, L.E. Erro 1, Tonantzintla, 72000 Puebla, Pue., Mexico

ARTICLE INFO

Article history:
Received 12 June 2008
Revised 10 September 2008
Available online 31 October 2008

Keywords:
Sagnac interferometer
Fibre-optic devices
Optical signal processing

ABSTRACT

A numerical study of a fibre-based scheme for the regeneration of ultrashort-pulsed optical signals is presented. The setup is made of a power-symmetric Nonlinear Optical Loop Mirror (NOLM) followed by a polariser. The NOLM operates through nonlinear polarisation rotation, and includes twisted, anomalous-dispersion fibre and a quarter-wave retarder. When the orientations of the linear input polarisation and of the output polariser are properly adjusted, the output energy characteristic flattens at high power, a property that can be used to eliminate large amplitude fluctuations on the logical ones of an optical signal. When the input pulse parameters closely match those of fundamental solitons or of stable elliptically polarised solitary waves, a wide and flat plateau is obtained, allowing the reduction of ~30% amplitude fluctuations to less than 1%. Very large amplitude fluctuations beyond 50% can also be reduced down to a few %. Although the output pulses are slightly chirped, they are free of pedestal, thanks to the zero low-power transmission of the NOLM, which also allows the simultaneous regeneration of logical zeros. We believe that this setup will be useful for the regeneration of highly degraded signals in future ultrafast transmission networks.

1. Introduction

In order to allow the transmission of data streams at 40 Gbits/s or beyond over long distances, all-optical signal regeneration techniques capable of handling ultrashort pulsed signals at very high rates will be needed in future transmission networks. The regeneration task includes the reduction of amplitude jitter on logical ones and the suppression of the optical power present on the logical zeros, which originates from amplifier noise, or from ghost pulses, for example.

Several fibre-based techniques were developed to tackle with these two problems. One of them is based on cascaded four-wave mixing in fibre [1–3], and another relies on self-phase modulation followed by offset filtering [4–6]. The first technique allows realising near-ideal step-like transfer functions, at the price however of a rather complicated setup, including one (or multiple) intense continuous-wave pump, and a phase or frequency modulation scheme for both signal and pump in order to suppress stimulated Brillouin scattering. Another inconvenient of the technique is that the wavelength of the regenerated signal differs from the initial signal wavelength. The latter technique also allows high-quality regeneration, and usually leads to simpler regenerator structures, as no pump source is needed. However the regenerated signal is also wavelength-shifted. Two stages are needed for wavelength-shift-free regeneration, which complicates the setup [7].

The fibre Nonlinear Optical Loop Mirror (NOLM) [8], which exploits the ultrafast nonlinear Kerr effect in silica fibre, is a simple and versatile device which can also be used for this task [9]. Its transmission characteristic $T(P_{in}) = P_{out}/P_{in}$ is typically a sinusoidal function of power, which is minimal a low power and reaches a maximum at high power. This implies that the output power characteristic $P_{out} = TP_{in}$ grows slowly at low power, a property that can be exploited for noise reduction on the zeros or pedestal suppression [10], and presents a maximum at high power, slightly beyond the transmission maximum, which can be used to reduce amplitude fluctuations on logical ones [11]. This maximum is not very extended however, as only the first derivative of P_{out} cancels out at this point, and only allows the suppression of relatively small amplitude fluctuations, whereas somewhat larger fluctuations are imperfectly eliminated due to the concavity of the characteristic [11]. Large amplitude fluctuations can be suppressed however using a strongly power imbalanced setup, in which a 0.9/0.1 coupler is employed, as for this particular coupling ratio an extended plateau appears in the P_{out} characteristic, where its first two derivatives cancel out simultaneously [12]. Amplitude

* Corresponding author.
E-mail address: pottiez@cio.mx (O. Pottiez).

1068-5200/$ – see front matter
doi:10.1016/j.yofte.2008.09.004

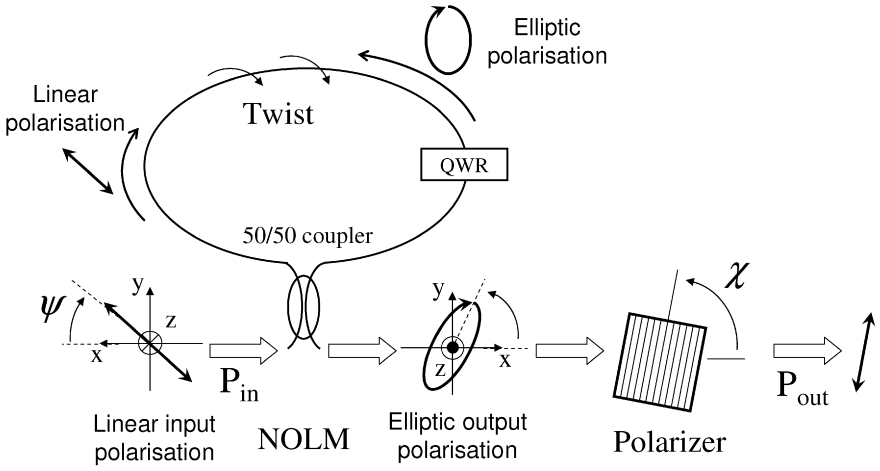

Fig. 1. Configuration under study.

fluctuations larger than 20% can be eliminated using this setup. In a previous work, we showed that a similar characteristic could be obtained using a power-symmetric architecture [13]. In both cases however, low-power transmission is high, yielding poor noise reduction on the zeros. On the other hand, a NOLM designed for zero regeneration yields poor performance for the regeneration of ones, as already mentioned. In general, a NOLM-based setup for signal regeneration includes several stages [14].

In a previous work [15], we showed that a setup based on a power-symmetric, nonlinear polarisation rotation (NPR)-based NOLM and a polariser could be used to generate a characteristic presenting a wide plateau at high power, without having to sacrifice the zero low-power transmission of the NOLM. The NOLM operates through a polarisation asymmetry instead of a power asymmetry between the counter-propagating beams. The polarisation states of counter-propagating beams are made different through the use of a quarter-wave retarder (QWR) inserted in the loop after one of the coupler output ports. To prevent the nonlinear polarisation evolution from averaging out for each beam during propagation, twist is applied to the fibre, which then becomes optically active and behaves like an ideal isotropic fibre [16]. Previous efforts to describe the device operation all relied on a continuous-wave model [17,18], which also yields quite accurate predictions for large pulses (with durations higher than, say 10 ps). Substantial differences are to be expected however in the ultrashort (∼ps) pulse regime, when chromatic dispersion and group velocity mismatch between polarisation components play an important role. In this case, where nonlinear phase shift and polarisation no longer vary only with power but also with time across the pulse, the properties of the above mentioned plateau will critically depend on the input pulse properties. Actually, the very existence of this plateau could be jeopardised.

Since the NOLM invention, numerous numerical studies were carried out to analyse the device operation in the ultrashort pulse regime. In the case of anomalous dispersion, these studies showed the outstanding properties of solitons, which can be switched entirely with minimal pulse shape distortion [8,19], and demonstrated the capabilities of the device for pulse compression and shaping [20,21], pedestal removal [10] or soliton stabilisation over long transmission links [22]. However, most of these studies used a scalar approach, neglecting the polarisation effects which play nevertheless an important role, in the continuous-wave as well as in the ultrashort pulse regimes. In the latter case in particular, the physics of solitons is modified when polarisation effects are taken into account. For example, in an isotropic fibre, solitons in the strict sense do not exist for states of polarisation other than linear or circular. In spite of this, only a few studies of polarisation effects in NOLMs can be found in the literature [18,23–25], most of which do not investigate in detail the ultrashort pulse regime.

In this paper, we analyse numerically the operation of the NPR-based NOLM followed by a polariser in the ultrashort pulse regime. Dispersion is anomalous, and pulses with sech^2 intensity profiles are considered. The properties of the plateau that can be generated in the output energy characteristic of the device are discussed in function of the duration of the input pulses.

2. Numerical analysis

The setup is presented in Fig. 1. It includes a NOLM followed by a polariser. The NOLM consists of a symmetrical coupler, a quarter-wave retarder (QWR) and a piece of circularly birefringent fibre. The QWR causes the beams to have different polarisations, whereas circular birefringence (obtained through twist) ensures that these polarisations are maintained over the whole fibre length. The loop has a length $L = 1$ km, an anomalous dispersion value $D = 19$ ps/nm/km ($\beta_2 = -24.2$ ps^2/km at 1550 nm), and a nonlinear coefficient for linear polarisation $\gamma = 7.5$ W^{-1} km^{-1}. The continuous-wave NOLM minimal switching power can be calculated as $P_\pi = 6\pi/\gamma L = 2.51$ W (note that, in previous works [15], a factor of 4 instead of 6 appears in the expression of P_π, as in that case the nonlinear coefficient, defined for circular polarisation, was $\beta = 2/3\gamma$, yielding $P_\pi = 4\pi/\beta L$). The parameters were chosen in order to ensure that a NOLM with relatively moderate length could properly switch pulses having their duration in the picosecond range for a peak power not higher than a few watts. Input polarisation is linear, and its angle ψ (defined with respect to one of the QWR axes) can be adjusted. At the NOLM output, a polariser making an angle χ with the QWR selects one of the linear polarisation components of the emerging pulse.

In practise, circular birefringence can be obtained in a standard silica fibre simply by applying twist. Twist has two effects. First, it rotates the fibre birefringence axes, so that the fibre residual birefringence, whose beat length $L_B \approx 10$–50 m [26,27], is easily averaged out by a moderate twist of 1 turn/m or less. A second effect is the generation of optical activity, causing light polarisation to rotate at ∼5% of the twist rate [18,28]. When the fibre is wound on a spool after twisting, the stress-induced birefringence axes do not rotate with twist, whereas the polarisation rotates with respect to these axes at only ∼0.05 times the twist rate, so that the averaging out of birefringence is less effective in this case. However, it was shown that, if the radius of curvature is kept sufficiently

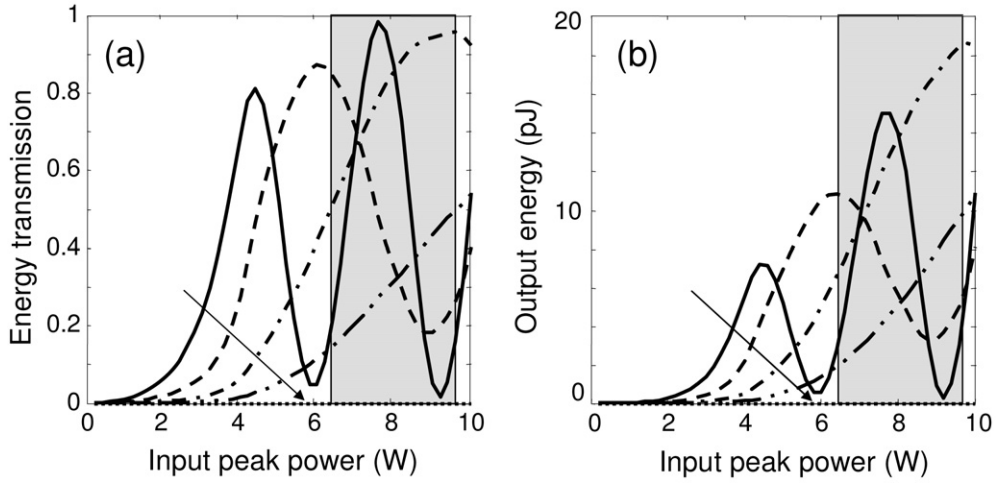

Fig. 2. (a) Transmission and (b) output energy characteristics of the NOLM for various values of $\psi = \pi/4$, $0.4\pi/4$, $0.2\pi/4$, $0.1\pi/4$ and 0 (in the sense of the arrows). FWHM input pulse duration $T_{\mathrm{FWHM}} = 1.8$ ps. Shaded box materialises the interval between the peak powers for which the CW and the CCW pulses are fundamental solitons when $\psi = \pi/4$ (6.46 W and 9.68 W, respectively).

large (say, 30 cm), a moderate twist rate of 1 turn/m can still be sufficient to ensure nearly circular birefringence [16]. On the other hand, for large values of twist (e.g., 5–10 turns/m), we observed through numerical simulations that ultrashort pulses are severely distorted by the group velocity mismatch between their two circular polarisation components. In particular, pulses at the NOLM output present a strong asymmetry and are substantially widened with respect to the case of moderate twist, even though at high power the polarisation components remain bound together during propagation thanks to the interplay between dispersion and Kerr effect, and the pulses do not split [29]. For this reason, high twist has poor practical interest for our purposes and, in this study, we consider a circularly birefringent fibre loop with a moderate twist of 1 turn/m. In this case, the simulated results show no substantial difference with respect to an ideal isotropic fibre loop, even in the ultrashort pulse regime.

To study the NOLM operation in the ultrashort pulse regime, the coupled nonlinear Schrödinger equations are used [29]. In the basis of circular polarisation $[C^+, C^-]$, they write as

$$\frac{\partial C^+}{\partial z} = -\frac{\Delta\beta_1}{2}\frac{\partial C^+}{\partial t} - j\frac{\beta_2}{2}\frac{\partial^2 C^+}{\partial t^2} + \frac{2j\gamma}{3}\left(|C^+|^2 + 2|C^-|^2\right)C^+;$$
$$\frac{\partial C^-}{\partial z} = +\frac{\Delta\beta_1}{2}\frac{\partial C^-}{\partial t} - j\frac{\beta_2}{2}\frac{\partial^2 C^-}{\partial t^2} + \frac{2j\gamma}{3}\left(|C^-|^2 + 2|C^+|^2\right)C^-, \qquad (1)$$

where $\Delta\beta_1 = \beta_1^+ - \beta_1^-$ is the inverse group velocity mismatch. Time t is referenced in a system that travels at the group velocity $v_g = 2/(\beta_1^+ + \beta_1^-)$. Note that, for circular polarisation, the self-phase modulation (SPM) coefficient is 2/3 times smaller than the SPM coefficient γ for linear polarisation. Fibre loss is neglected, as well as higher-order dispersion and Raman self-frequency shift, a valid approximation for the parameters of the NOLM and of the pulses considered here. The split-step Fourier technique is used to numerically integrate these equations for both the clockwise (CW) and counter-clockwise (CCW) beams.

The continuous-wave analysis of the NPR-based NOLM [30] showed that, for particular values of the QWR orientation, low-power transmission = 0. In order to ensure maximal extinction ratio enhancement, the QWR is maintained in such a position. In this case, the switching characteristic is a sinusoidal function of input power, which grows from 0 at low power and reaches 1 for some nonzero value of power, called the switching power, P_π. The value of P_π depends on the angle ψ of input polarisation with the QWR. This comes from the fact that, whereas the CW beam is always linearly polarised, the polarisation of the CCW beam is generally elliptic, and depends on ψ. If $\psi = \pi/4$, the CCW polarisation is circular after passing the QWR, the polarisation asymmetry between CW and CCW beams is maximal, and P_π is minimal. If now $\psi = 0$, both beams are linearly polarised, no nonlinear phase shift difference appears and transmission does not grow with power ($P_\pi = \infty$). Hence, in continuous-wave operation, the NOLM switching power can be adjusted between a minimal value and infinity simply by adjusting the input polarisation orientation.

In the case of ultrashort pulses, as expected, the inclusion of dispersion substantially modifies the quantitative results. The qualitative behaviour however remains the same as above, as shown in Fig. 2, where the transmission T_N and output pulse energy E_{out} characteristics of the NOLM are presented, for various values of the input polarisation orientation. The transmission is here defined as the ratio between the pulse energies at the NOLM output and input, respectively, $T_N = E_{\mathrm{out}}/E_{\mathrm{in}}$. Maximal transmission is no longer = 1, as low-power skirts of the pulse do not transmit well through the NOLM, except when the counter-propagating pulses turn out to be close to solitons, with a nonlinear phase shift nearly constant across the pulse profile (shaded box in Fig. 2).

The continuous-wave description of the NOLM also allowed studying the output polarisation in function of the input power and polarisation, and of the NOLM parameters [30]. In particular, for linear input polarisation, the ellipticity (ratio between minor and major axes) of the output polarisation was shown to be independent of power, and to depend on the input polarisation angle ψ. When ψ is close to 0, output polarisation is close to linear. As ψ increases, the output ellipticity gradually increases, until polarisation becomes circular for $\psi = \pi/4$. For a given input polarisation orientation, the output ellipticity is not modified as power is increased, although the ellipse rotates proportionally to power. These results suggest that, if a polariser is placed at a given orientation χ after the NOLM output, its transmission T_P will vary sinusoidally with power. The amplitude of this variation is related with the NOLM output ellipticity (and thus with ψ), whereas the position of its maxima and minima (its phase) can be adjusted through the polariser orientation χ. By adjusting ψ and χ, it is possible to obtain a T_P characteristic that flattens the maximum of T_N, so that the resulting output power characteristic presents a wide plateau, where the first three derivatives cancel out simultaneously [15].

In this work, we intend to generalise this principle to the ultrashort pulse regime. More specifically, the goal is to show nu-

merically that it is possible, using a NPR-based NOLM followed by a polariser, to obtain a flat plateau in the resulting output power characteristic, $E_{out} = T_N T_P E_{in}$, and to analyse its characteristics, like its width and flatness. One important aspect is that, in general, the output state of polarisation will now vary across the pulse profile, which complicates the analysis. As it will appear later, interesting properties appear when the pulses propagating in the loop are close to solitons, so that we will analyse this case with some detail. In a nearly isotropic fibre, first-order ($N = 1$) solitons only exist for linear and circular polarisations, having in each case different width-height products [31], a fact that can be understood by considering that the nonlinear coefficient $= \gamma$ in the former case and $2/3\gamma$ in the latter case. In both cases, the pulse will suffer no alteration during propagation, in particular its polarisation (linear or circular) will remain constant across the profile. Strictly speaking, however, no elliptic solitons exist, and there is no way that an initial uniformly elliptically polarised pulse can propagate without deformation. Nevertheless, some solitary wave solutions were found for elliptic polarisation in an isotropic fibre, one of which is stable [31]. For this solution, the polarisation state is not constant across the pulse, but constitutes a fixed pattern that rotates as the pulse propagates, in quite the same way as for continuous-wave light. As the polarisation is not constant across the pulse, the pulse profiles of the two circular polarisation components are different: the lower-amplitude component is slightly shorter than the stronger one. This solution however only slightly differs from a squared hyperbolic secant pulse with uniform elliptic polarisation, as it will appear in the following.

Even though elliptic solitons can not be defined, let us look for a condition under which a squared hyperbolic secant pulse with uniform elliptic polarisation across its profile undergoes minimal deformation during propagation (except for a global nonlinear rotation of the polarisation ellipse). In this case, as in first approximation only one polarisation state is involved, the problem can be considered as scalar, and the scalar soliton theory can be applied. The properties of such "approximate solitons" depend on the nonlinear coefficient for that particular state of polarisation, which can be extracted from the continuous-wave propagation equations. Let us rewrite Eq. (1) with $\Delta\beta_1$ and $\beta_2 = 0$ as:

$$\frac{\partial C^+}{\partial z} = \frac{2j\gamma}{3}\left(|C^+|^2 + 2|C^-|^2\right)C^+ = \frac{2j\gamma}{3}P\left(\frac{3}{2} - \frac{1}{2}A_c\right)C^+;$$
$$\frac{\partial C^-}{\partial z} = \frac{2j\gamma}{3}\left(|C^-|^2 + 2|C^+|^2\right)C^- = \frac{2j\gamma}{3}P\left(\frac{3}{2} + \frac{1}{2}A_c\right)C^-, \qquad (2)$$

where $P = |C^+|^2 + |C^-|^2$ is the optical power and $A_c = |C^+|^2 - |C^-|^2/P$ is the first Stokes parameter. Let us now define an elliptic polarisation basis $[S^+, S^-]$, with $S^+ = \cos\alpha C^+ + \sin\alpha C^-$ and the orthogonal polarisation vector $S^- = -\sin\alpha C^+ + \cos\alpha C^-$, where $0 \leqslant \alpha \leqslant \pi/2$ and let us consider a pure S^+ input polarisation. Using Eq. (2), $A_c = (\cos\alpha)^2 - (\sin\alpha)^2$ and some trigonometric identities, the equation for the evolution of S^+ is given by

$$\frac{\partial S^+}{\partial z} = \frac{2j\gamma}{3}P\left[\left(1 + \frac{1}{2}\sin^2(2\alpha)\right)S^+ + \frac{1}{2}\cos(2\alpha)\sin(2\alpha)S^-\right]. \qquad (3)$$

The first term in Eq. (3) corresponds to SPM, whereas the second term is responsible for NPR [16]. The first term allows to define a nonlinear coefficient for the S^+ polarisation,

$$\gamma_\alpha = \frac{2}{3}\gamma\left(1 + \frac{1}{2}\sin^2(2\alpha)\right) = \gamma\left(1 - \frac{1}{3}\cos^2(2\alpha)\right) = \gamma\left(1 - \frac{1}{3}A_c^2\right).$$

For linear ($\alpha = \pi/4$) and circular ($\alpha = 0$ or $\pi/2$) input polarisations, this formula yields the well-known coefficients $\gamma_\alpha = \gamma$ and $\gamma_\alpha = 2/3\gamma$, respectively. In analogy with exact solitons, the elliptically polarised pulse will undergo minimal deformation if its peak power P_0 and full width at half maximum (FWHM) duration T_{FWHM} verify $N^2 = \gamma_\alpha P_0 (T_{FWHM}/1.763)^2/|\beta_2| = 1$, where β_2 is the dispersion parameter of the fibre.

We simulated the propagation along a fibre with anomalous dispersion of a hyperbolic secant pulse with uniform elliptic polarisation, and whose peak power P_0 and full width at half maximum (FWHM) duration T_{FWHM} verify $N^2 = \gamma_\alpha P_0 (T_{FWHM}/1.763)^2/|\beta_2| = 1$. For convenience, throughout this text we will refer to the value of N calculated using the above formula as the "soliton order," although it is clear that no soliton is formed when N is not an integer, and that no soliton in the strict sense exist for elliptic polarisation. As shown in Fig. 3(a), after 1 km of propagation ($\sim$7 soliton periods), only minor changes affect the pulse profile. In particular, changes are barely visible in the stronger circular polarisation component. As to the small-intensity component, its duration is slightly decreased and its peak power is correspondingly increased, as the pulse evolved towards the stable solitary wave described in [31]. Besides, the phase remains constant over most of the pulse width, in quite the same way as it happens for solitons. Fig. 3(b) further confirms that the polarisation remains nearly the same across the pulse, except in the low-intensity wings [Fig. 3(c)]. After propagation, the ellipticity near the pulse centre is also nearly the same as at the input [except for a global nonlinear rotation of the pattern, see thick arrow in Fig. 3(b)]. In summary, although they are not strictly invariant during propagation, elliptic sech^2 pulses undergo minimal distortion and remain approximately unchirped and uniformly polarised as they propagate when $N = 1$.

The above analysis suggests that, if the pulses that counterpropagate in the NOLM loop are solitons or elliptic sech^2 pulses with $N = 1$, the generation of a wide flat plateau in the characteristic of the NOLM with output polariser is still possible, as in this case the pulses behave essentially like in the continuous-wave case, with overall nonlinear phase shift and polarisation rotation and almost no variation of phase and polarisation across the pulse. It should be noted however that, although they have equal powers due to the 50/50 coupler, the soliton order N_{CW} of the linearly polarised CW beam and the order N_{CCW} of the elliptically polarised CCW beam cannot be simultaneously $= 1$, as the nonlinear coefficients are different for these two polarisations. For a given input polarisation orientation ψ, the ellipticity of the CCW beam after the QWR is determined by $\alpha = \pi/4 - \psi$, which allows the calculation of the corresponding nonlinear coefficient γ_α. If both N_{CW} and N_{CCW} are sufficiently close to 1, however, although different, pulse distortions are small and the analogy with the continuous-wave case still applies.

We showed in [15] that, in the continuous-wave case, if the input polarisation and polariser angles are properly adjusted, a plateau appears for a particular value of power, which is slightly beyond the switching power. In the case of solitons, the input peak power is also imposed by the nonlinear phase shift needed to reach the plateau. If the pulses injected in the loop in each direction are close to solitons ($N_{CW}, N_{CCW} \approx 1$), their duration is thus imposed as well, through the relation existing between peak power and duration. Fig. 4 shows the results obtained for an input pulse with duration $T_{FWHM} = 2.3$ ps. It can be seen in Fig. 4(b) that, for proper adjustment of ψ and χ, a wide plateau appears at an input peak power of $\sim$4.3 W. The figure also shows that, for this duration, the interval over which the soliton orders of the counterpropagating beams are close to 1 ($N_{CCW} < 1 < N_{CW}$, shaded area) is centred with the plateau. At the power of the plateau centre ($\sim$4.3 W), the pulse profiles thus undergo minimal distortions during propagation along the loop. If the average peak power of the input pulses is 4.3 W, energy fluctuations of $\sim$30% can be reduced to $\sim$1% at the polariser output. Fig. 4(c) presents the time-bandwidth product (TBP) of the output pulses (solid curve), as well as the TBP of the transform-limited (TL) pulses having the

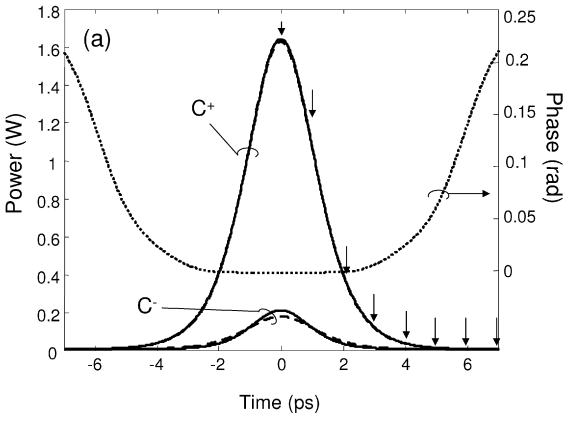

(a)

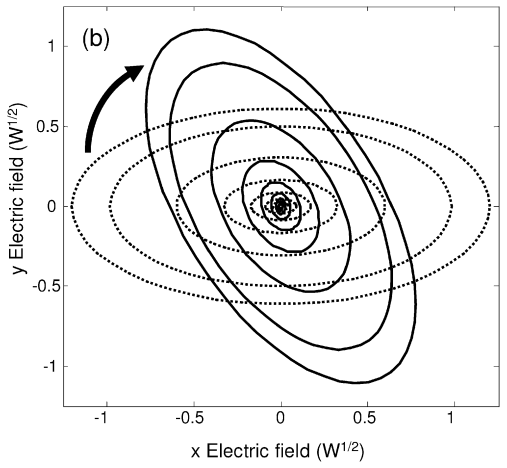

(b)

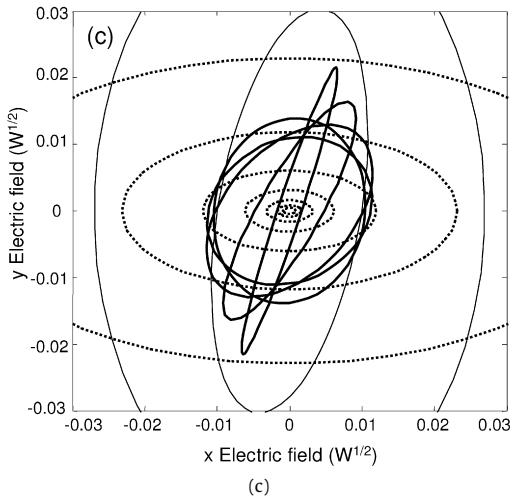

(c)

Fig. 3. (a) Power profiles of C^+ and C^- components of an elliptically polarised sech^2 pulse prior to (dashed) and after (solid) propagation through 1 km of fibre; the phase profile of the output pulse is also represented (dotted line); (b) polarisation state at various positions across the pulse profile [arrows in part (a)], prior to (dotted) and after (solid) propagation; (c) detail of part (b), where thick solid lines show the output polarisation in the profile skirt at 8, 9, 10, 11 and 12 ps away from the peak. Initial pulse duration $T_{\mathrm{FWHM}} = 2.65$ ps, $\alpha = 0.4\pi/4$, $D = 19$ ps/nm/km, and $\gamma = 7.5\ \mathrm{W^{-1}\,km^{-1}}$.

same temporal profile as the actual output pulses (dashed curve). Note that even the TBP of the TL pulses varies with input power: even if the considered input profile is invariably a sech^2, the output pulse profile varies with input peak power (in particular, the reduction of the TBP of the TL pulses at the high power end of Fig. 4(c) is related to pedestal formation). Over the extension of the plateau, the TBP of the output pulses is around 0.3, although the TBP of the TL pulses is smaller, indicating the presence of some chirp in the actual pulses. The difference between the two curves is minimal however at the plateau. Fig. 4(d) shows the soliton order of the output pulse, for linear polarisation. The output soliton order does not present strong variations across the plateau, and is quite close to 1. Finally, Fig. 4(e) shows the "pedestal," calculated as the relative difference in modules between the output pulse energy and the energy of the squared hyperbolic secant pulse having the same T_{FWHM} and peak power as the actual pulse. A pedestal tends to form when the pulses injected in the loop depart from fundamental solitons. In the present case, the pedestal does not amount to more than a few %, as the zero low-power transmission of the NOLM ensures efficient pedestal suppression [Fig. 4(a)]. At the plateau centre, where N_{CW} and $N_{\mathrm{CCW}} \approx 1$, the pedestal reaches its minimal value of ~0.7%. Away from the plateau, however, the output pulse presents a substantial pedestal, as the pedestals accompanying each of the counter-propagating pulses are different and do not cancel out when they interfere at the NOLM output.

To illustrate the regenerative action of the device, Figs. 4(f) and 4(g) show an example of eye diagrams obtained at the regenerator input ant output, respectively, after filtering the signal in each case using a Gaussian bandpass filter with 1.25-nm FWHM bandwidth. 2.3-ps sech^2 pulses are used to form a 40-Gb/s return-to-zero on-off keyed (RZ-OOK) signal. The input signal is degraded by a substantial amount of Gaussian amplitude noise, as shown by Fig. 4(f). Fig. 4(g) shows that the noise on both marks and spaces is strongly reduced at the device output.

Fig. 5 shows the transmission and output energy characteristics of the NOLM and polariser for different values of the input pulse duration. Again, ψ and χ are adjusted so as to get a "plateau" as flat as possible in the output energy characteristic (in the case of ψ, the optimal adjustment is found to be roughly the same for all values of T_{FWHM}). When $T_{\mathrm{FWHM}} \neq 2.3$ ps, the soliton orders of the CW and CCW pulses are no longer close to 1 for peak power values corresponding to the plateau. In this case, and as far as the soliton orders do not get close to another integer ($0.5 < N < 1.5$), each pulse evolves during propagation to adjust its parameters to reach $N = 1$. This takes a few soliton periods. With the parameters of this study, and over the range of pulse duration considered (1.8 ps $< T_{\mathrm{FWHM}} <$ 3.5 ps), the soliton period is included between ~65 m and ~260 m, so that this evolution is nearly completed in all cases after the 1-km propagation in the loop. For each input pulse duration, the input peak power at the plateau centre will have a value such that the average peak power of the pulses (which will vary during propagation) corresponds to the nonlinear phase shift needed to reach the plateau. If $T_{\mathrm{FWHM}} < 2.3$ ps, it appears in Figs. 5(b) and 5(d) that the input peak power at the plateau is higher than in the case of Fig. 4, and the soliton orders are smaller (<1). Indeed, in this case, the pulses widen and their peak powers are reduced during propagation as their soliton orders get close to 1. When pulses are shorter, their input peak power is thus higher, which ensures that the same average peak power is maintained over propagation. If now $T_{\mathrm{FWHM}} > 2.3$ ps, Figs. 5(f) and 5(h) show that the input peak power at the plateau is lower than in the case of Fig. 4, and that the soliton orders are larger (>1). This can be understood by considering that the pulses in this case will get shorter during propagation, and their peak power higher, in order to reduce the soliton number. The input peak power is thus reduced for longer pulses in order to maintain the same average peak power corresponding to the plateau.

As in the cases presented in Fig. 5 the soliton numbers of the injected pulses are not close to 1 at the plateau, the pulses suffer substantial readjustments during propagation, so that one may expect some differences with respect to the case of Fig. 4. Fig. 6

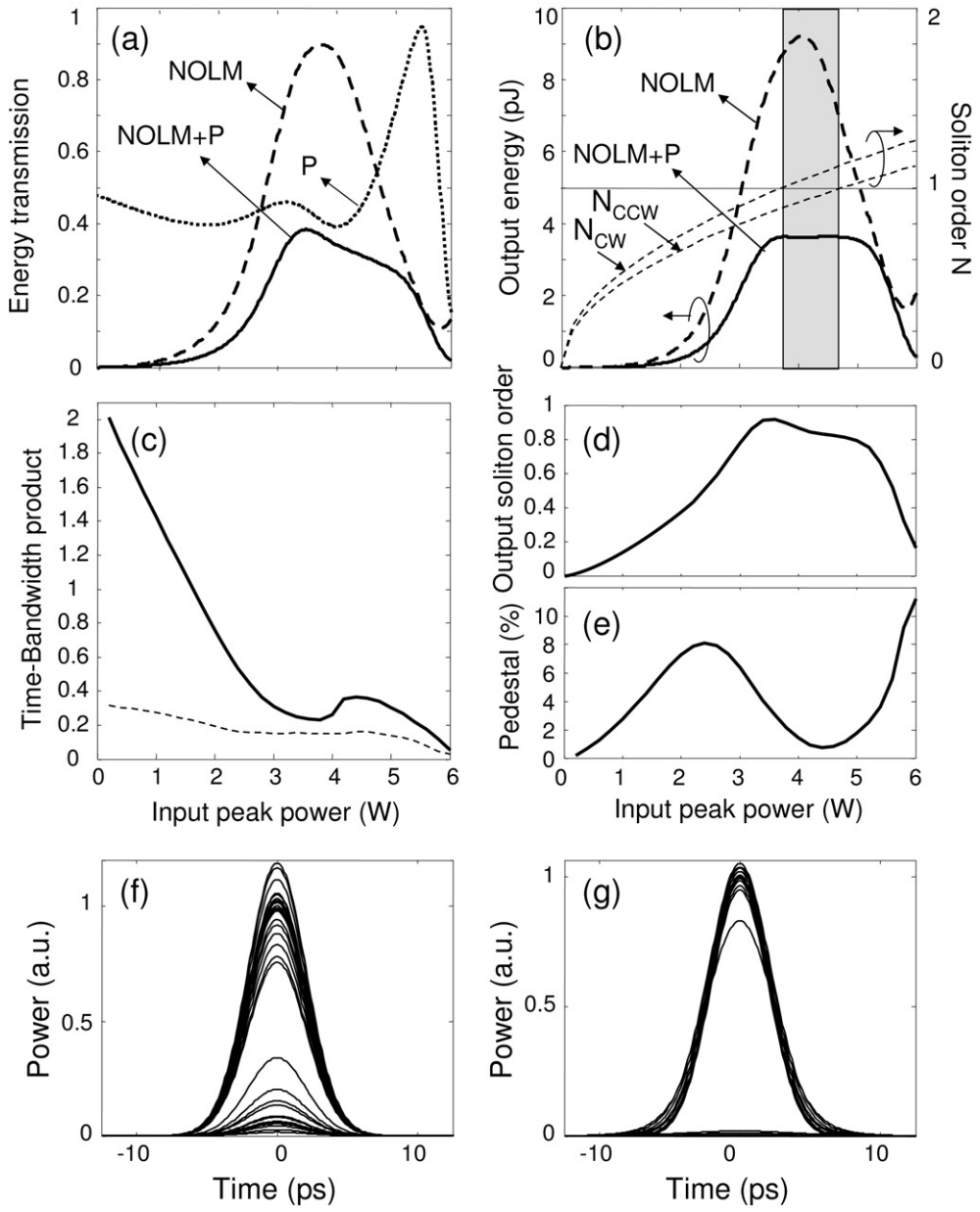

Fig. 4. (a) Transmission and (b) output energy characteristics of the NOLM and of the NOLM followed by the polariser (NOLM+P). The polariser (P) transmission is also included in part (a), and the soliton orders of the CW and CCW pulses when they are injected in the loop are shown in part (b); (c) time–bandwidth product of the NOLM+P output pulses (solid) and of the transform-limited pulses (dashed); (d) output soliton order and (e) pedestal of the output pulses, as functions of input peak power; (f, g) eye diagrams obtained at the regenerator input and output, respectively, for a 40-Gb/s signal with Gaussian amplitude noise and average input peak power = 4.3 W (a Gaussian bandpass filter with 1.25-nm FWHM bandwidth was used). Input pulse duration $T_{FWHM} = 2.3$ ps, $\psi = 0.59\pi/4$ and $\chi = 0.82$.

shows the plateau width as a function of input pulse duration, for several values of the maximal residual energy fluctuation tolerated at the device output. This width is thus defined as the maximal relative energy fluctuation of the input pulses that can be reduced to a particular value, assuming that the average input peak power is adjusted at the plateau centre. Fig. 6 shows that, for the smaller values of input pulse duration, the plateau width is relatively small [see also Figs. 5(b) and 5(d)]. Imposing the output fluctuation to be no more than 1%, the plateau width drops suddenly beyond $T_{FWHM} = 2.3$ ps, showing that a maximum is obtained for this duration. For this duration, the soliton orders are close to 1 for both pulses as they are injected in the loop, so that they quickly stabilise with minor adjustments of their parameters. So the widening of the plateau and its excellent flatness that occur for this value of pulse duration appear to be a manifestation of the stability of solitons [29] and of solitary waves [31]. For smaller durations, the plateau width is reduced, although its flatness is maintained. When the duration is increased however, flatness is degraded, due to the appearance of some ripple on the plateau, causing a sudden decay of the plateau width when the amplitude of this ripple becomes larger than the tolerated output fluctuation. In particular, for $T_{FWHM} = 3.35$ ps [Fig. 5(h)] or higher, one may actually consider that no plateau is obtained, except if a residual amplitude fluctuation of more than 10% is acceptable. This ripple appearing for larger values of pulse duration can be understood by considering that the soliton period is larger for larger pulse durations. For this reason, when the pulses injected in the loop substantially depart from $N = 1$, the pulse profile is not yet perfectly stabilised after propagating through the loop. Simulations show that the pulse parameters (peak power, duration, polarisa-

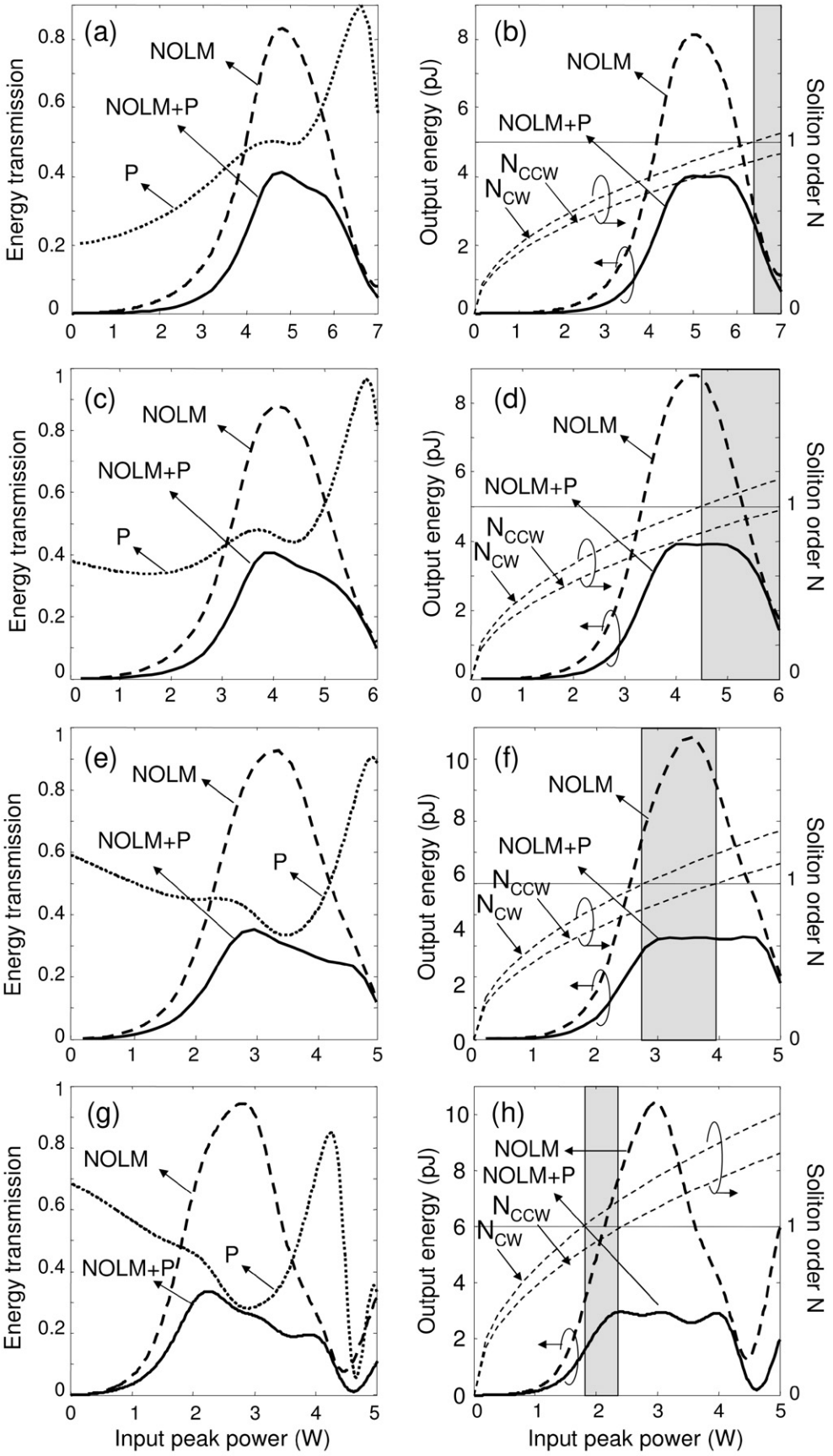

Fig. 5. (a, c, e, g) Transmission and (b, d, f, h) output energy characteristics of the NOLM, the polariser (P) and of the NOLM followed by the polariser (NOLM+P). The polariser (P) transmission is also included in parts (a, c, e, g), and the soliton orders of the CW and CCW pulses when they are injected in the loop are shown in parts (b, d, f, h). Input pulse durations are $T_{FWHM} = 1.76$ ps (a, b), 2.11 ps (c, d), 2.68 ps (e, f) and 3.35 ps (g, h); $\psi = 0.59\pi/4$ (a, b, c, d), $0.61\pi/4$ (e, f), $0.64\pi/4$ (g, h); $\chi = 1.58$ (a, b), 0.99 (c, d), 0.62 (e, f), 0.40 (g, h).

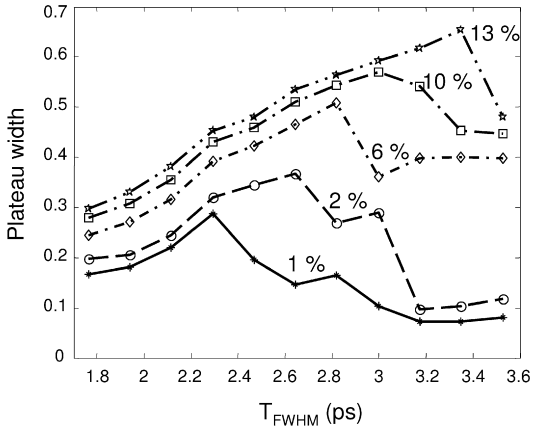

Fig. 6. Plateau width as a function of input pulse duration, for various values of the output amplitude fluctuation (indicated as curve labels).

tion) oscillate with the propagation distance, and the pulse profile reached at the fibre end substantially varies with small changes on the input conditions, like the input peak power. These oscillations of the pulse parameters thus induce the ripple observed in the plateau for large input pulse duration. If now a residual output fluctuation amplitude higher than 1% is tolerated, Fig. 6 shows that the plateau width is not significantly modified for small pulse duration. However, the maximum plateau width is larger, and occurs for larger pulse duration. Beyond this maximum, the plateau width drops again, as the ripple becomes too large. This shows that, as the pulse width is increased, the plateau extension increases, at the price of an increase in the ripple. If the tolerance on the output amplitude fluctuation is substantially relaxed, very large amplitude fluctuations beyond 50% can be reduced.

Although the best regeneration performances are obtained in the case of sech^2 pulses, simulations showed that a plateau can also be obtained in the output energy characteristic using other pulse profiles. In particular, Gaussian profiles can be used. For a FWHM duration of 2.3 ps, for example, the pulses adapt their shapes to ideal sech^2 profiles as they propagate along the loop, although this evolution is accompanied by the formation of a substantial dispersive background accompanying each pulse. For proper adjustments of ψ and χ, a plateau appears in the output energy characteristic. Although its width and flatness are reduced in comparison with the soliton case, it still allows the reduction of ~25% peak-to-peak amplitude fluctuations on the marks to 2%. Finally, at very high bit rates, as the successive bits begin to overlap, the device operation is limited by the interaction between solitons. Simulations show however that, for the pulse duration of 2.3 ps, this problem does not appear for data rates as high as 40 and even 80 Gb/s. For operation at higher rates (160 Gb/s), pulses as short as ~1 ps should be used, and the NOLM design has to be adapted to this value of pulse duration.

It has to be noted finally that linear input polarisation with the prescribed orientation should be strictly maintained at the NOLM input for the device to operate in the wide plateau regime. A polarised signal from a sufficiently narrow bandwidth source conserves its 100% degree of polarisation even after propagation through long spans of standard fibre (i.e., no random polarisation appears), however the polarisation state at the end of the link is subject to continuous erratic changes due to slow variations of the fibre residual birefringence, which is due to environmental (temperature and mechanical) disturbances. Fortunately, as polarisation-sensitive devices are common in optical telecommunications (in particular integrated devices), schemes were soon developed to actively stabilise the polarisation state at the output of a fibre link [32–35], and they can also be implemented to ensure proper operation of the regenerating device proposed in this paper. Basically, these schemes rely on the measurement of polarisation at the fibre end; this information is then used in a feedback loop to manipulate controllable birefringent elements (e.g., squeezers) disposed along the fibre, in order to maintain the desired output polarisation state.

3. Conclusion

We performed a numerical study of a device composed of a NPR-based NOLM and a polariser to regenerate ultrashort-pulsed optical signals whose signal-to-noise ratio is strongly deteriorated. The NOLM operates in the anomalous dispersion regime, and a moderate torsion is applied to the fibre in order to ensure a nearly isotropic medium. If the orientations of the linear input polarisation and of the output polariser are properly adjusted, a flat plateau appears in the output energy characteristic of the device, allowing the reduction of amplitude noise on logical ones. When the parameters of the pulses injected in the loop closely match those of a first-order soliton or of an elliptically polarised solitary wave, a wide plateau with an excellent flatness is obtained. In this case, amplitude fluctuations as large as 30% can be reduced to ~1% using this scheme. The plateau extension can be increased, at the price however of a ripple appearing on the plateau and reducing its flatness. Fluctuations as large as 43% can then be reduced to 2.5%, and fluctuations beyond 50% can be reduced down to 6%. As the orientation of the QWR inserted in the NOLM is adjusted for zero low-power transmission, the device also allows the reduction of noise on the logical zeros or of low-powered ghost pulses, like in the case of a conventional NOLM. Although the output pulses are slightly chirped, they are close to fundamental solitons and are linearly polarised. We believe that the proposed scheme will be useful for signal-to-noise ratio and extinction enhancement of ultrafast data trains in future high-speed optical transmission systems.

Acknowledgment

O. Pottiez was supported by CONACyT grant 53990.

References

[1] S. Yamashita, M. Shahed, Optical 2R regeneration using cascaded fiber four-wave mixing with suppressed spectral spread, IEEE Photon. Technol. Lett. 18 (2006) 1064–1066.
[2] E. Ciaramella, F. Curti, S. Trillo, All-optical signal reshaping by means of four-wave mixing in optical fibers, IEEE Photon. Technol. Lett. 13 (2001) 142–144.
[3] S. Radic, C.J. McKinstrie, R.M. Jopson, J.C. Centanni, A.R. Chraplyvy, All-optical regeneration in one- and two-pump parametric amplifiers using highly nonlinear optical fiber, IEEE Photon. Technol. Lett. 15 (2003) 957–959.
[4] P.V. Mamyshev, All-optical data regeneration based on self-phase modulation effect, in: Proc. European Conference on Optical Communications, Madrid, Spain, 1998, pp. 475–476.
[5] T.-H. Her, G. Raybon, C. Headley, Optimization of pulse regeneration at 40 Gb/s based on spectral filtering of self-phase modulation in fiber, IEEE Photon. Technol. Lett. 16 (2004) 200–202.
[6] M. Matsumoto, Performance analysis and comparison of optical 3R regenerators utilizing self-phase modulation in fibers, J. Lightwave Technol. 22 (2004) 1472–1482.
[7] M. Matsumoto, Efficient all-optical 2R regeneration using self-phase modulation in bidirectional fiber configuration, Opt. Express 14 (2006) 11018–11023.
[8] N.J. Doran, D. Wood, Nonlinear-Optical Loop Mirror, Opt. Lett. 13 (1988) 56–58.
[9] S. Boscolo, S.K. Turitsyn, K.J. Blow, Nonlinear Loop Mirror-based all-optical signal processing in fiber-optic communications, Opt. Fiber Technol. 14 (2008) 299–316.
[10] M.D. Pelusi, Y. Matsui, A. Suzuki, Pedestal suppression from compressed femtosecond pulses using a nonlinear fiber loop mirror, IEEE J. Quantum Electron. 35 (1999) 867–874.
[11] M. Attygalle, A. Nirmalathas, H.F. Liu, Novel technique for reduction of amplitude modulation of pulse trains generated by subharmonic synchronous mode-locked laser, IEEE Photon. Technol. Lett. 14 (2002) 543–545.

[12] M. Meissner, R. Rösch, B. Schmauss, G. Leuchs, 12 dB of noise reduction by a NOLM-based 2-R regenerator, IEEE Photon. Technol. Lett. 15 (2003) 1297–1299.
[13] O. Pottiez, E.A. Kuzin, B. Ibarra-Escamilla, F. Gutiérrez-Zainos, U. Ruiz-Corona, J.T. Camas-Anzueto, High-order amplitude regularization of an optical pulse train using a power-symmetric NOLM with adjustable contrast, IEEE Photon. Technol. Lett. 17 (2005) 154–156.
[14] A. Bogoni, P. Ghelfi, M. Scaffardi, L. Potì, All-optical regeneration and demultiplexing for 160-Gb/s transmission systems using a NOLM-based three-stage scheme, IEEE J. Select. Top. Quantum Electron. 10 (2004) 192–196.
[15] O. Pottiez, B. Ibarra-Escamilla, E.A. Kuzin, High-quality amplitude jitter reduction and extinction enhancement using a power-symmetric NOLM and a polarizer, Opt. Express 15 (2007) 2564–2572.
[16] T. Tanemura, K. Kikuchi, Circular-birefringence fiber for nonlinear optical signal processing, J. Lightwave Technol. 24 (2006) 4108–4119.
[17] S.F. Feldman, D.A. Weinberger, H.G. Winful, Polarization instability in a twisted birefringent optical fiber, J. Opt. Soc. Am. B 10 (1993) 1191–1201.
[18] E.A. Kuzin, N. Korneev, J.W. Haus, B. Ibarra-Escamilla, Theory of nonlinear loop mirrors with twisted low-birefringence fiber, J. Opt. Soc. Am. B 18 (2001) 919–925.
[19] M.N. Islam, E.R. Sunderman, R.H. Stolen, W. Pleibel, J.R. Simpson, Soliton switching in a fiber nonlinear loop mirror, Opt. Lett. 14 (1989) 811–813.
[20] L. Chusseau, E. Delevaque, 250-fs optical pulse generation by simultaneous soliton compression and shaping in a nonlinear optical loop mirror including a weak attenuation, Opt. Lett. 19 (1994) 734–736.
[21] I.Y. Khrushtchev, I.H. White, R.V. Penty, High-quality laser diode pulse compression in dispersion-imbalanced loop mirror, Electron. Lett. 34 (1998) 1009–1010.
[22] N.J. Smith, N.J. Doran, Picosecond soliton transmission using concatenated nonlinear optical loop-mirror intensity filters, J. Opt. Soc. Am. B 12 (1995) 1117–1125.
[23] N. Finlayson, B.K. Nayar, N.J. Doran, Switch inversion and polarization sensitivity of the nonlinear-optical loop mirror, Opt. Lett. 17 (1992) 112–114.
[24] C. Baskev Clausen, J.H. Povlsen, K. Rottwitt, Polarization sensitivity of the nonlinear amplifying loop mirror, Opt. Lett. 21 (1996) 1535–1537.
[25] Q. Lin, G.P. Agrawal, Impact of fiber birefringence on optical switching with nonlinear optical loop mirrors, IEEE J. Select. Top. Quantum Electron. 10 (2004) 1107–1114.
[26] A. Galtarossa, L. Palmieri, M. Schiano, T. Tambosso, Measurements of beat length and perturbation length in long single-mode fibers, Opt. Lett. 25 (2000) 384–386.
[27] E.A. Kuzin, J.M. Estudillo-Ayala, B. Ibarra-Escamilla, J.W. Haus, Measurements of beat length in short low-birefringence fibers, Opt. Lett. 26 (2001) 1134–1136.
[28] R. Ulrich, A. Simon, Polarization optics of twisted single-mode fibers, Appl. Opt. 18 (1979) 2241–2251.
[29] G.P. Agrawal, Nonlinear Fiber Optics, third ed., Academic Press, San Diego, 2001.
[30] O. Pottiez, E.A. Kuzin, B. Ibarra-Escamilla, F. Mendez-Martinez, Theoretical investigation of the NOLM with highly twisted fibre and a $\lambda/4$ birefringence bias, Opt. Commun. 254 (2005) 152–167.
[31] Y. Silberberg, Y. Barad, Rotating vector solitary waves in isotropic fibers, Opt. Lett. 20 (1995) 246–248.
[32] R. Ulrich, Polarization stabilization on single-mode fiber, Appl. Phys. Lett. 35 (1979) 840–842.
[33] P. Granestrand, L. Thylen, Active stabilisation of polarisation on a single-mode fibre, Electron. Lett. 20 (1984) 365–366.
[34] R. Noe, H. Heidrich, D. Hoffmann, Endless polarization control systems for coherent optics, J. Lightwave Technol. 6 (1988) 1199–1208.
[35] J. Chen, G. Wu, Y. Li, E. Wu, H. Zeng, Active polarization stabilization in optical fibers suitable for quantum key distribution, Opt. Express 15 (2007) 17928–17936.

Olivier Pottiez was born in 1974 in Beloeil, Belgium. He received the Electrical Engineer and PhD degrees from the Faculté Polytechnique de Mons (FPMs, Mons, Belgium) in 1997 and 2001, respectively. In 2003, he realised a postdoctoral stay at the Instituto Nacional de Astrofísica, Óptica y Electrónica (INAOE, Puebla, Mexico). He is currently a researcher in the Fibre Optics Department of the Centro de Investigaciones en Óptica (CIO, León, Mexico). His present research interests include mode-locked fibre lasers for ultrashort pulse generation and fibre Sagnac interferometers for ultrafast photonics applications.

Baldemar Ibarra-Escamilla was born in Veracruz, Mexico, on April 9, 1969. He received the Bachelor degree in Electronics from the Benemerita Universidad Autonoma de Puebla, Mexico, in 1994. He received the M.S. and Ph.D. degrees in optics from the Instituto Nacional de Astrofísica, Optica y Electrónica (INAOE), Mexico, in 1996 and 1999, respectively. During 2000 he did a postdoctoral stay at the Electro-Optics Graduate Program, University of Dayton, USA. He is currently a researcher of the Optics Department from the INAOE. His interests are in the field of optical fibre modelocked lasers, optical fibre amplifiers, tunable optical fibre lasers, and fibre-optic sensors.

Evgeny A. Kuzin was born in 1948 in St. Petersburg, Russia. He graduated from the University of St. Petersburg in 1976 and obtained the Ph.D. degree from the Phys-Technical Institute of Academy of Sciences of Russia in 1983. He was affiliated with the Phys-Technical Institute from 1976 to 1995, and since 1995 he is working at the National Institute of Astrophysics, Optics and Electronics, Puebla, Mexico.